Annual Methodological Archive Research Review
http://amresearchreview.com/index.php/Journal/about
Volume 4, Issue 5 (2026)

Online ISSN 3007-3197
Print ISSN 3007-3189

http://amresearchreview.com/index.php/Journal/about

Numerical Simulation Of Square Pin-Fin Heat Sink For Cooling Of Electronic Devices

Muhammad Zahid*(Corresponding Author)
Department of Mathematics and Statistics, University of Southern Punjab, Multan 66000, Pakistan. muhammadzahid82@gmail.com

Ajab Gul
Department of Mathematics and Statistics, University of Southern Punjab, Multan 66000, Pakistan

ABSTRACT

In this study, CFD simulations for a heat sink with square pin-fin for the purpose of cooling of electronic components of devices are executed. A heat sink is responsible for removing excessive heat from electronic components of devices while they are under operational conditions. The heat sink is placed in a duct with an inlet-outlet arrangement. The inlet velocity is the input parameter varying from 2 m/s to 12 m/s with a step of 2, while the output parameters are the Nusselt number and the heat sink base temperature for the performance measure. The flow model comprises three dimensional Navier-Stokes equations, the continuity and energy equations, along with two extra transport equations for capturing the turbulence. The turbulent model used is SST $k-\omega$ turbulence model. For solving the system of non-liner partial differential equation, we use finite volume method that gives approximate solution. All simulations are carried out on ANSYS Workbench. The heat source is a constant and uniform heat flux of q'' = 10000 Watt/m^2 at the base of the heat sink. The temperature of the heat sink base is high enough to be around 362.4 K when the inlet velocity is u = 2 m/s, while it is low enough to be around 320 K when the inlet velocity is u = 12 m/s. The results obtained are quite consistent with the physics of the problem.

Keywords— Heat sink, inlet velocity, Nusselt number, square-pin-fin, simulation

1. INTRODUCION

The rapid progress of modern technology has created a growing demand for highly efficient heat transfers systems because the modern technology is offering compact electronic components in very small volumes while their processing capabilities are very high. A rapid and excessive rise in temperature results in deformation or damage to these electronic components. To secure the systems from deformation or damage, the finned heat sinks are frequently used, where the fins, as extended surfaces, are a standard feature of these heat sinks used for heat dissipation and thermal exchange. Optimizing the heat transfer systems typically involve the design and flow parameters to be addressed. The design parameters involve fin size, fin density, fin spacing, fin shape, etc., while the operational parameters are the inlet mass flow rate, boundary

Annual Methodological Archive Research Review
http://amresearchreview.com/index.php/Journal/about
Volume 4, Issue 5 (2026)

Online ISSN 3007-3197
Print ISSN 3007-3189
http://amresearchreview.com/index.php/Journal/about

conditions, ambient temperature, etc. Some of the common cooling techniques utilize finned heat sinks and heat pipes [1-3]. The finned heat sinks are cheap and smart and so are popular among all the modern heat transfer techniques [4] where air is commonly used for convection. The types of heat sinks are based on fin designs. Several researchers have worked to evaluate the performance of these types of the heat sinks [5-7]. Nilpueng et al. [8] worked on experimental setup for investigating the impact of some design and operating parameters for investigating the performance of two different heat sinks. One is the sinusoidal wavy-plate-fin heat sinks and the other is manipulated by creating cross-cuts. They found that manipulated heat sinks performed better in terms of Nusselt number *Nu*. Tariq et al. [9] proposed heat sinks with perforations and slots. The perforations not only decrease the weight, but give improved performance.

The heat sinks with pin-fins are also under investigation extensively by various researchers [10-14]. A hybrid heat sink with pin-fins and a micro lattice structure was considered for numerical study by Wang et al. [15] for numerical investigations. The outcome of their investigations revealed that this hybrid approach causes lower pressure drop when compared with the existing heat sinks. A numerical study has been conducted by Soleymani et al. [16] for investigating the impact of some input parameters for investigating the performance of a pin-fin heat sink. The study revealed that rectangular round edged pin-fin heat sink gave improved thermal performance. Jonsson and Bjorn [17] conducted experimental studies for comparing the thermal performance of some heat sinks. The fins of the heat sinks include plate fins and pin-fins with different cross sections under the similar operational conditions. The performance of the elliptical pin-fin was recorded as better at high velocities while that of the circular pin-fin was recorded better for medium velocities. The experimental results of Wirtz et al. [18] for various pin-fin designs revealed that the performance of the cylindrical pin-fins was best. A similar work has also been conducted by [19-20] for investigating the thermal performance. Ahmadian et al. [21] performed numerical study using finite volume method for investigating the heat sinks with different pin-fin shapes. It was proven that the fin shape plays a critical role has a great impact on the convective heat transfer and pressure drop.

In the current manuscript, a square pin-fin heat sink made up of the aluminum is under consideration. The velocity at the inlet takes values from 2 m/s to 12 m/s with a step of 2, while the output parameters are *Nu* and temperature T_b of the heat sink base for the measuring the performance. The intention of the study is investigating an appropriate system comprising a square pin-fin heat sink offering a solution for cooling the electronic devices.

2. PROBLEM STATEMENT

The heat sink under consideration is a heat sink with square pin-fins, made up of the aluminum. The heat sink is placed in a rectangular duct with an inlet-outlet arrangement. The heat sink base is also a square shape with length and width each being 100 mm while its thickness is 3 mm. There are five fins in each row along the flow direction as well as across the flow direction, mounted on the heat sink base, thus there are 25 fins in total. The length of each edge of the base of the fin is 8 mm while height

Annual Methodological Archive Research Review
http://amresearchreview.com/index.php/Journal/about
Volume 4, Issue 5 (2026)

Online ISSN 3007-3197
Print ISSN 3007-3189
http://amresearchreview.com/index.php/Journal/about

of the fin is 50 mm. The length, width and height of the duct is 350 mm, 120 mm and 50 mm. There is a free passage of 100 mm between the inlet and the heat sink base while it is of 150 mm between the heat sink and the outlet. The inlet velocity is an input parameter that takes values from 2 m/s to 12 m/s with an increment of 2. The heat sink base is given a uniform constant heat flux q'' = 10000 Watt/m^2. The target variables are the Nusselt number *Nu* and the heat sink bas temperature T_b. The geometric model of this setup is given in Figure 1.

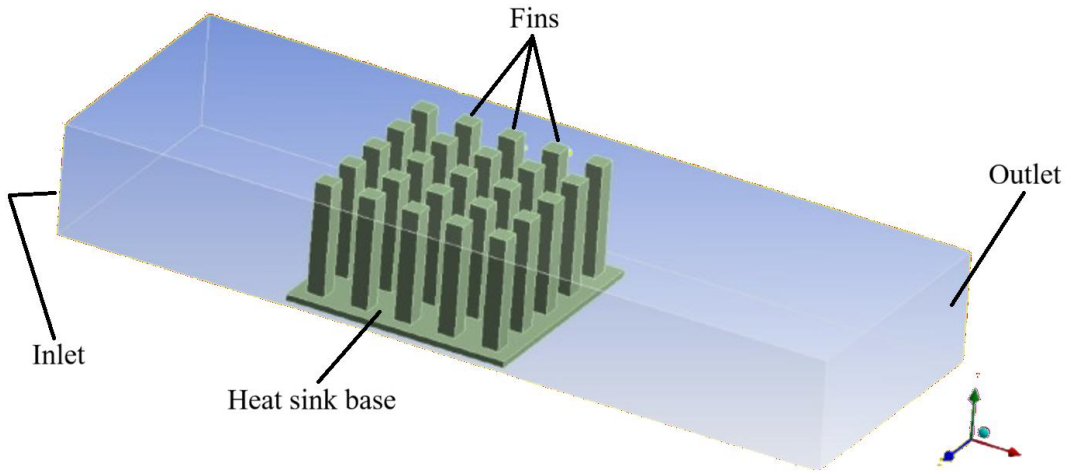

Figure 1. Computational domain comprising heat sink and duct with inlet-outlet arrangement.

3. MATHEMATICAL FORMULATION

In this section, we give some flow and heat transfer assumptions and the governing equations of the problem.

3.1 Flow and Heat Transfer Assumptions

(a) The problem is a steady, 3D, incompressible and turbulent.
(b) SST $k-\omega$ model is used for the turbulence.
(c) The problem is a conjugate heat transfer problem. The radiations are ignored.
(d) The thermo-physical properties of the materials are constant.
(e) The base of the heat sink is given a constant and uniform heat flux of q'' = 10000 Watt/m^2.
(f) The fin and the duct heights are equal to avoid flow bypass complexities.
(g) Symmetry boundary conditions are imposed on duct walls which considers zero gradients of velocity and temperature.

3.2 Mathematical Model

The mathematical model that governs the flow is

$$\nabla \cdot \vec{u} = 0, \tag{1}$$

$$\rho(\vec{u} \cdot \nabla)\vec{u} = -\nabla p + \mu \nabla^2 \vec{u}, \tag{2}$$

$$\rho c_p(\vec{u} \cdot \nabla T) = \nabla \cdot (\kappa \nabla T), \tag{3}$$

Annual Methodological Archive Research Review
http://amresearchreview.com/index.php/Journal/about
Volume 4, Issue 5 (2026)

Online ISSN 3007-3197
Print ISSN 3007-3189
http://amresearchreview.com/index.php/Journal/about

where $\vec{u}$, g, p, T and κ are the velocity vector, gravitational acceleration, pressure, temperature and material's thermal conductivity respectively.
The heat conduction in the heat sink is governed by the equation

$$\nabla \cdot (\kappa_s \nabla T) = 0 \quad (4)$$

The solid-fluid interface thermal conditions are given as follows.

$$T_s = T_f, \quad (5)$$

$$\kappa_s \frac{\partial T_s}{\partial n} = \kappa_f \frac{\partial T_f}{\partial n} \quad (6)$$

The base of the heat sink is given uniform constant heat flux

$$q'' = -\kappa_s \frac{\partial T}{\partial n} = 10000\ Watt/m^2 \quad (7)$$

The boundary conditions are as under.

The inlet velocity conditions are as under,

$$u = 2,\ 4,\ 6,\ 8,\ 10,\ 12,\quad T = 300\,K. \quad (8)$$

The outlet is given zero gauge pressure as

$$p = 0,\ \frac{\partial u}{\partial n} = 0,\ \frac{\partial T}{\partial n} = 0. \quad (9)$$

On duct walls, symmetry boundary conditions are imposed which consider zero gradients of velocity and temperature, i.e.,

$$\frac{\partial u}{\partial n} = 0,\ \frac{\partial T}{\partial n} = 0. \quad (10)$$

3.3 Turbulence Model

In the current study, SST $k-\omega$ turbulence model is used for the turbulence modeling, which solves two additional transport equations given below along with the transport equations of the general flow model given by Equations (1)-(3),

$$\rho(u \cdot \nabla k) = \nabla \cdot \left[\left(\mu + \frac{\mu_t}{\sigma_k} \right) \nabla k \right] + \tilde{G}_k - \rho \beta^* f_{\beta^*} k\omega, \quad (11)$$

$$\rho(u \cdot \nabla \omega) = \nabla \cdot \left[\left(\mu + \frac{\mu_t}{\sigma_\omega} \right) \nabla \omega \right] + \frac{\gamma}{\nu_t} G_k - \rho \beta f_\beta \omega^2 + D_\omega, \quad (12)$$

where D_ω is the cross-diffusion term which is the critical term that blends the $k-\omega$ and $k-\varepsilon$ models.

4. SOLUTION PROCEDURE

We solve the conjugate heat transfer problem numerically using finite volume method which is built-in in ANSYS Fluent 16.2. All the tasks of simulations, i.e., geometry creation, meshing, choice of models, solution and postprocessing have been performed

Annual Methodological Archive Research Review
http://amresearchreview.com/index.php/Journal/about
Volume 4, Issue 5 (2026)

Online ISSN 3007-3197
Print ISSN 3007-3189
http://amresearchreview.com/index.php/Journal/about

using ANSYS Workbench. For solution, SIMPLE scheme is used for the pressure-velocity coupling., the Green-Gauss Cell-Based method is used for the gradient calculations, second order interpolation is used for the pressure for enhanced accuracy, and second order upwind scheme is used for the momentum, energy and turbulence. The first order upwind is used for the turbulence dissipation. The threshold for the residuals is set to below 10^{-3} for all the model equations except energy equation for which it is 10^{-6}.

5. COMPUTATIONAL MESH

The computational mesh of the computational domain is given in Figure 2 which contains 185199 nodes and 885030 elements. The mesh at the interfaces is the conformal mesh which means that the heat sink-body and the fluid-body share the same faces at the interfaces. This is an indicator of better accuracy of the results to be obtained. The maximum skewness of the mesh elements is recorded to be 0.89156, the maximum orthogonal quality to be 0.99806 and the maximum aspect ratio to be 28.834. These metrices confirm the quality of the mesh is good enough.

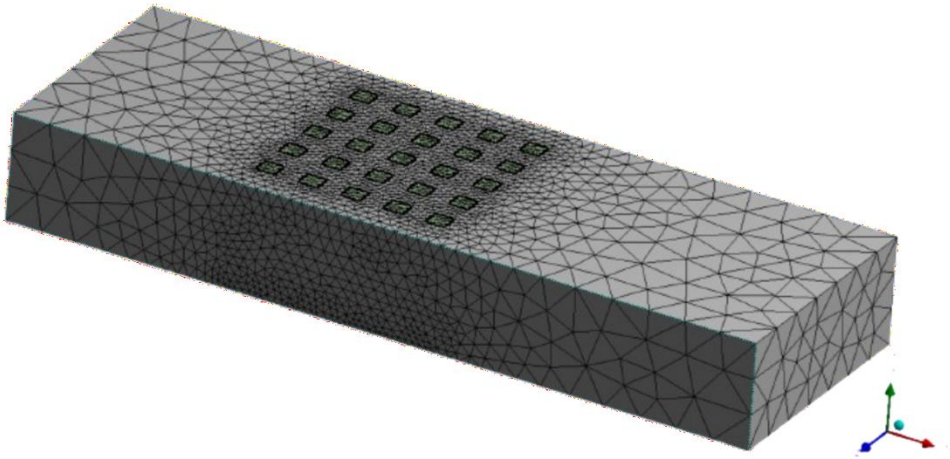

Figure 2. Mesh of the computational model.

6. RE SULTS AND DISCUSSION

In this section, we give details discussion of the influence of the inlet velocity u on the target variables, the Nu and the T_b.

6.1 Steady Thermal Parametric Response

In Figure 3, Nu is plotted against u. The Nu is the ratio of the convective heat transfer to the conductive heat transfer and is computed as

$$Nu = \frac{q''L}{\kappa(T_s - T_\infty)}, \tag{13}$$

where L is the characteristic length and T_∞ is the ambient fluid temperature. If $Nu > 1$, it is an indicator of convective enhanced flow. The graph clearly shows that the Nu is increasing with an increase in u. The graph is nonlinear in a way that the rate of change of Nu is decreasing with increase in u. This shows that if we continue to increase the

Annual Methodological Archive Research Review
http://amresearchreview.com/index.php/Journal/about
Volume 4, Issue 5 (2026)

Online ISSN 3007-3197
Print ISSN 3007-3189

http://amresearchreview.com/index.php/Journal/about

value of u, the Nu curve becomes asymptotic.

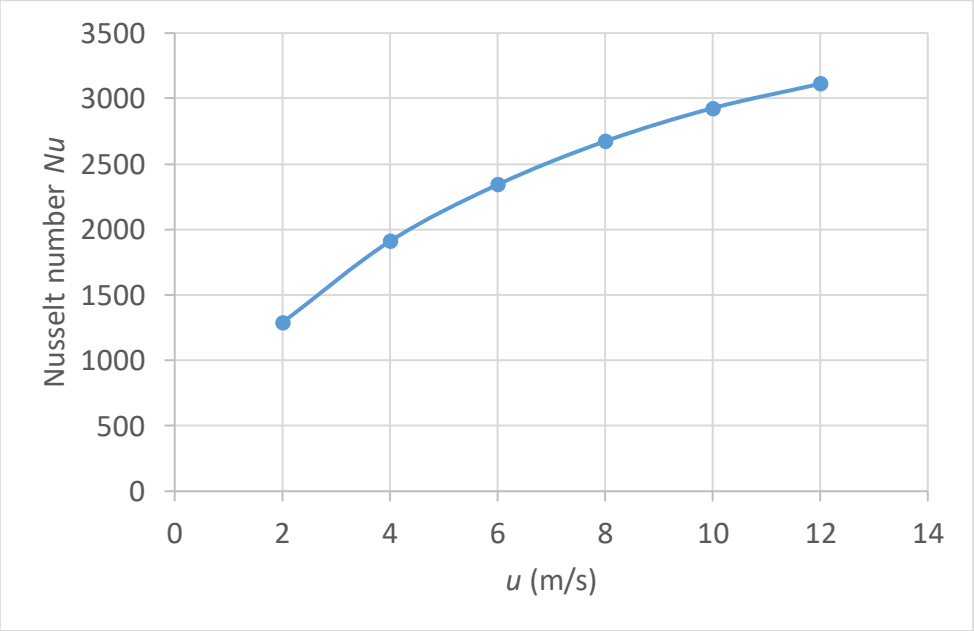

Figure 3. Nu curve against the inlet velocity u.

In Figure 4, T_b is plotted against u. The graph is highly nonlinear and shows that the temperature initially decreases quickly. As the value of u increases the decline in the T_b slows down. We can observe from the graph that when u changes from 2 m/s to 4 m/s, the change in T_b is about 22 degrees, while the change in T_b is about only 2 degrees when u changes from 10 m/s to 12 m/s. Here is again an asymptotic behavior if we continue to increase the value of u.

Annual Methodological Archive Research Review
http://amresearchreview.com/index.php/Journal/about
Volume 4, Issue 5 (2026)

Online ISSN 3007-3197
Print ISSN 3007-3189

http://amresearchreview.com/index.php/Journal/about

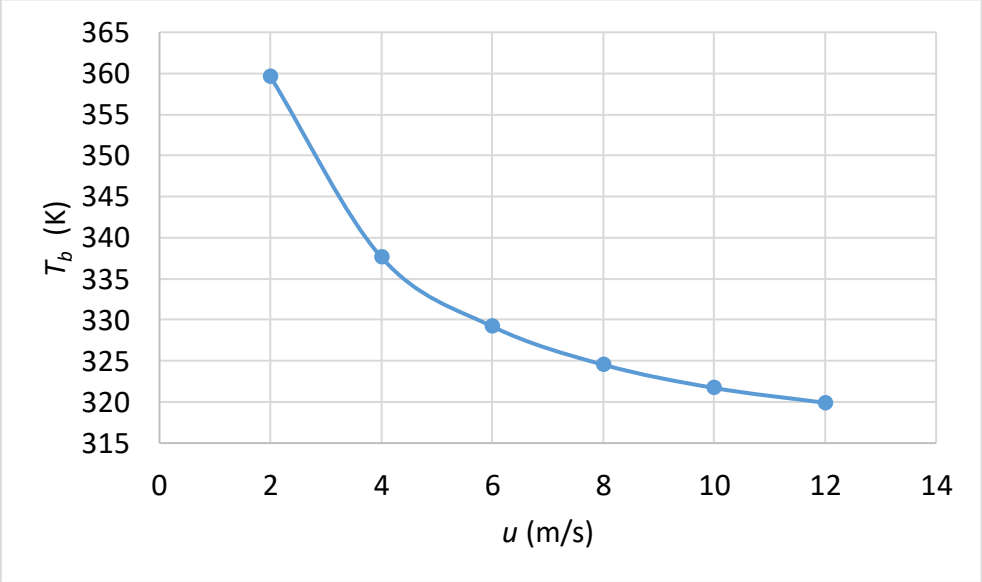

Figure 4. Temperature curve against the inlet velocity u.

In Figure 5, the pressure drop is plotted against u and this graph is also a nonlinear. The graph initially rises slowly, but it rises quickly as the value of u increases further. We can observe from the graph that when u changes from 2 m/s to 4 m/s, the change in pressure drop is about 16 Pascal, while its rise is around 50 Pascal when u changes from 10 m/s to 12 m/s. The pressure drop is the operational cost in the form of pumping power.

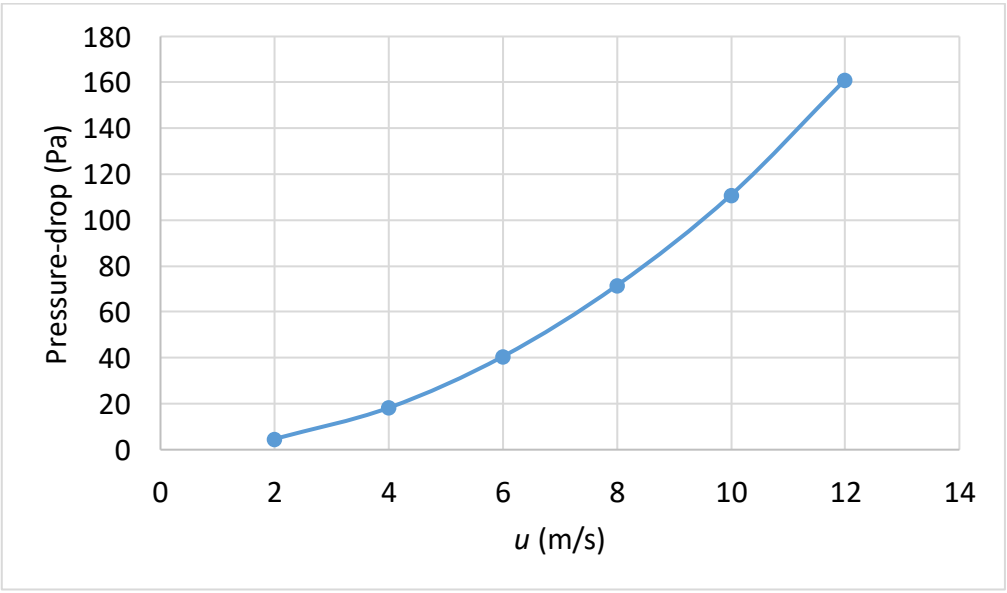

Figure 5. Pressure-drop curve against the inlet velocity u.

The overall discussion shows that the operational cost in terms of pressure drop is very

Annual Methodological Archive Research Review
http://amresearchreview.com/index.php/Journal/about
Volume 4, Issue 5 (2026)

Online ISSN 3007-3197
Print ISSN 3007-3189
http://amresearchreview.com/index.php/Journal/about

low against the smaller values of u, but it does not sufficiently cool the heat sink base. For a higher value of u = 12 m/s, the T_b is below 320 K (47 °C) and it is a safe temperature for CPUs. If we increase u further, the cost to benefit ratio will be very high and it will not be feasible. The proposed design is acceptable for the current scenario. If it is required to decrease the T_b further, the other design parameters may be incorporated to update the heat sink design, like number of fins, fin spacing, fin size, etc.

6.2 Spatial Thermal and Flow Analysis: Contour Analysis

In this subsection, we analyze the heat transfer process locally with the help of contours graphs. We plot the contour graphs in a vertical and a horizontal plane for the case u = 12 m/s. Plane-1 is the vertical plane, which is parallel to the xy-plane with an offset of z = 60 mm (center of the domain). Plane-2 is the horizontal plane, which is parallel to zx-plane with an offset of y = 25 mm (center of fins along their height). The detailed discussion on contour graphs is as under.

In Figure 6(a)&(b), the contour graphs of velocity are plotted in Plane-1 and Plane-2. The velocity at the inlet is clearly 12 m/s. When air comes across the fins of the heat sink, it changes its direction, and hence there is a wake behind each fin. There is a minimal flow in these wake areas because of the air coming around the fins. In Figure 6(b), we see that when air comes across the fins, the air velocity is maximum in the spaces between the fin rows along the flow direction. This indicates the momentum shift from the fin region to the open spaces.

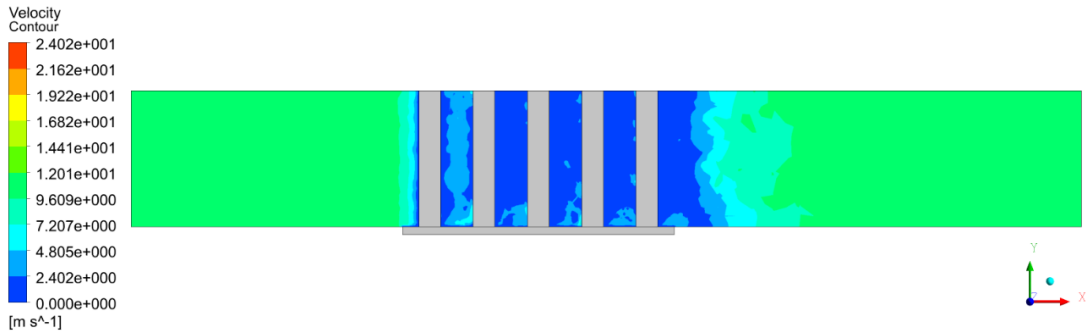

(a)

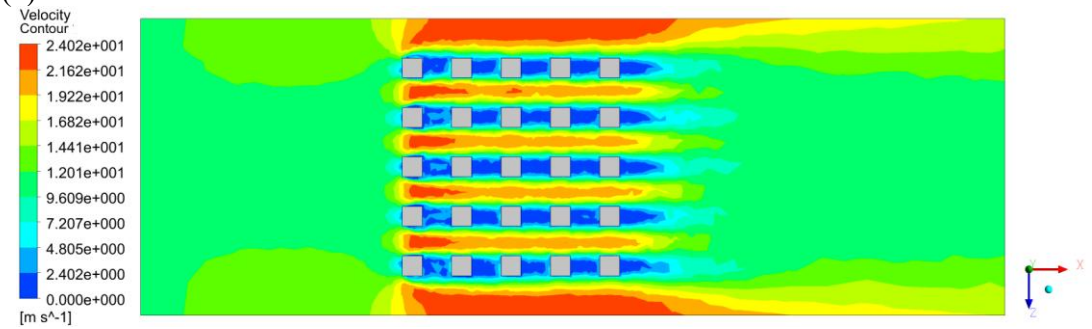

(b)

Figure 6. Velocity contours (a) Plane-1 and (b) Plane-2.

Annual Methodological Archive Research Review
http://amresearchreview.com/index.php/Journal/about
Volume 4, Issue 5 (2026)

Online ISSN 3007-3197
Print ISSN 3007-3189
http://amresearchreview.com/index.php/Journal/about

In Figure 7, the temperature contours of the heat sink surfaces are given. It is clear from the figure that the fins and the base on the left side of the heat sink are cooler than that of the right side. This is because the cool air coming from the left which gradually becomes hot while passing around the hot fins of the heat sink. Therefore, a nonuniform heat spread is seen in the heat sink.

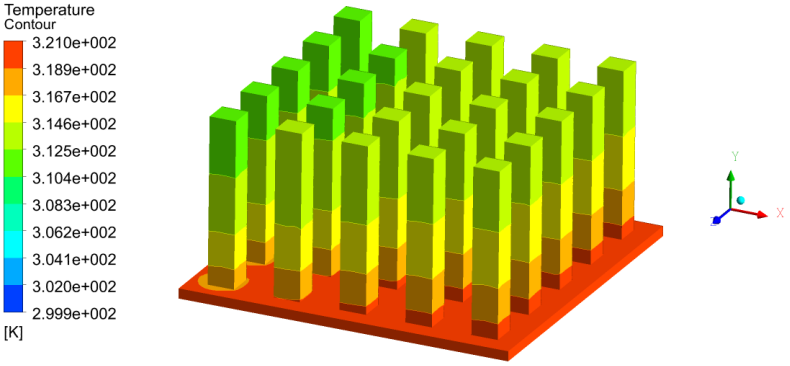

Figure 7. Temperature contours of heat sink surfaces, an isometric view.

In Figure 8(a)&(b), temperature contours are plotted in Plane-1 and Plane-2. These figures also supporting the arguments discussed in discussion of the Figures (6) and (7).

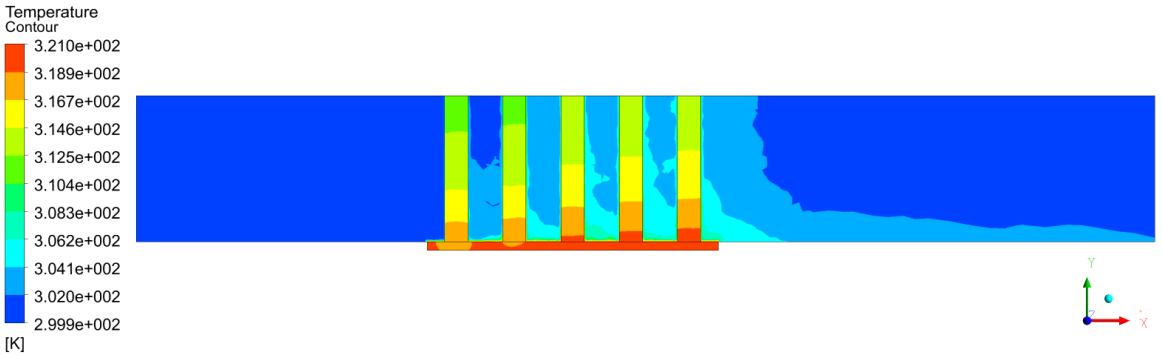

(a)

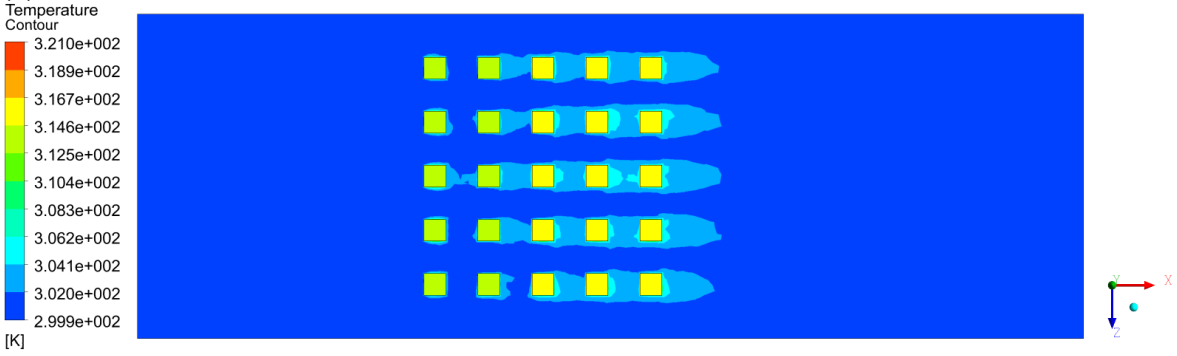

(b)

Figure 8. Temperature contours (a) Plane-1 and (b) Plane-2.

In Figure 9(a)&(b), pressure contours are plotted in Plane-1 and Plane-2. The air comes across the fins of the heat sink and strikes with all the fins in first row which is in the direction normal to the air flow. Due to the stagnation points, the velocity is minimum

Annual Methodological Archive Research Review
http://amresearchreview.com/index.php/Journal/about
Volume 4, Issue 5 (2026)

Online ISSN 3007-3197
Print ISSN 3007-3189
http://amresearchreview.com/index.php/Journal/about

in front of each fin, while the pressure is maximum here. The contours pattern is normal around the other fins and pressure is lower. This is why the air passes rapidly through the spaces between fins along the flow direction. The argument is supported by the streamline pattern given in Figure 10.

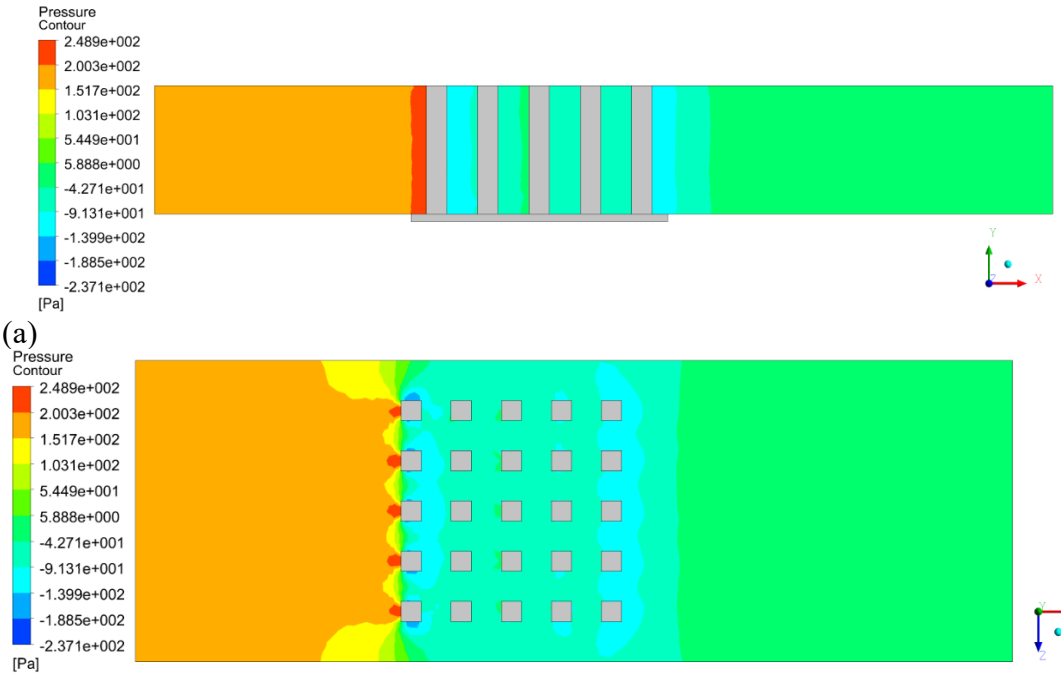

Figure 9. Pressure contours (a) Plane-1 and (b) Plane-2.

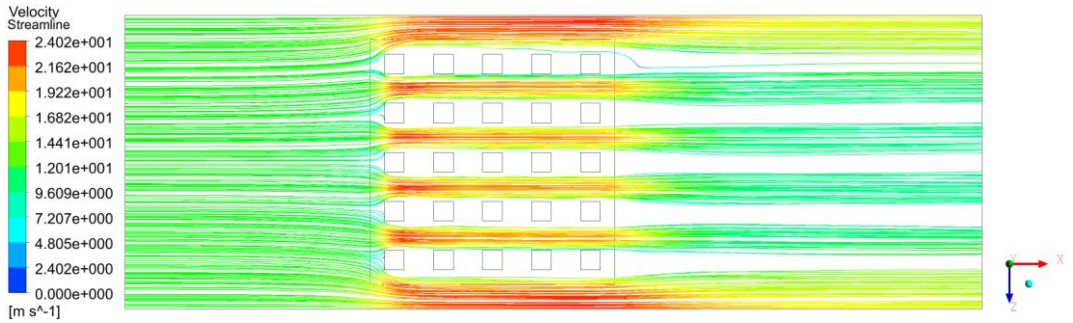

Figure 10. Velocity streamlines.

7. CONCLUSIONS

The current study explores investigation of the performance of a square-pin-fin heat sink for electronic components cooling under operational conditions. The inlet velocity varies from 2 m/s to 12 m/s with a step of 2. The heat sink base is given a heat flux boundary condition of q'' = 10000 Watt/m^2, while the output parameters are the

Annual Methodological Archive Research Review
http://amresearchreview.com/index.php/Journal/about
Volume 4, Issue 5 (2026)

Online ISSN 3007-3197
Print ISSN 3007-3189

http://amresearchreview.com/index.php/Journal/about

Nusselt number Nu and the heat sink base temperature T_b for the performance measure. The findings of the present work are:

1. The operational cost in terms of pressure drop is very low against the smaller values of u, but it does not cool the heat sink base sufficiently.
2. For a higher value of u = 12 m/s, the T_b is below 320 K (47 ºC) and it is a safe temperature for CPUs.
3. If we increase u further, the cost to benefit ratio will be very high and it will not be feasible.
4. The proposed design is acceptable for the current scenario. If further decrease in base temperature T_b is required, the other design parameters might be incorporated to update the heat sink design, like number of fins, fin spacing, fin size, etc.

References

[1] Sertkaya, A. A., & Sarı, S. (2021). Experimental investigation of heat transfer depending on inclination angle of unfinned, axial finned and radial finned heat exchangers. *International Journal of Heat and Mass Transfer*, *165*, Article 120704. https://doi.org/10.1016/j.ijheatmasstransfer.2020.120704.

[2] Kang, Z., Shou, D., & Fan, J. (2021). Numerical study of a novel single-loop pulsating heat pipe with separating walls within the flow channel. *Applied Thermal Engineering*, *196*, Article 117246. https://doi.org/10.1016/j.applthermaleng.2021.117246.

[3] Deng, D., Zeng, L., & Sun, W. (2021). A review on flow boiling enhancement and fabrication of enhanced microchannels of microchannel heat sinks. *International Journal of Heat and Mass Transfer*, *175*, Article 121332. https://doi.org/10.1016/j.ijheatmasstransfer.2021.121332.

[4] Vilarrubí, M., Riera, S., Ibañez, M., Omri, M., Laguna, G., Fréchette, L., & Rosell, J. I. (2018). Experimental and numerical study of micro-pin-fin heat sinks with variable density for increased temperature uniformity. *International Journal of Thermal Sciences*, *132*, 424–434. https://doi.org/10.1016/j.ijthermalsci.2018.06.019.

[5] Al-Sallami, W., Al-Damook, A., & Thompson, H. M. (2021). A numerical investigation of the thermal-hydraulic characteristics of perforated plate fin heat sinks. *International Journal of Thermal Sciences*, *121*, 266–277. https://doi.org/10.1016/j.ijthermalsci.2017.07.022.

[6] Yazici, M. Y., Avci, M., & Aydin, O. (2019). Combined effects of inclination angle and fin number on thermal performance of a PCM-based heat sink. *Applied Thermal Engineering*, *159*, Article 113956. https://doi.org/10.1016/j.applthermaleng.2019.113956.

[7] Chingulpitak, S., Seon, H., Godson, L., & Wongwises, S. (2019). Fluid flow and heat transfer characteristics of heat sinks with laterally perforated plate fins. *International Journal of Heat and Mass Transfer*, *138*, 293–303. https://doi.org/10.1016/j.ijheatmasstransfer.2019.04.027.

[8] Nilpueng, K., Seon, H., D. Jerng, & Wongwises, S. (2019). Heat transfer and flow characteristics of sinusoidal wavy plate fin heat sink with and without

Online ISSN 3007-3197
Print ISSN 3007-3189

crosscut flow control. *International Journal of Heat and Mass Transfer*, *137*, 565–572. https://doi.org/10.1016/j.ijheatmasstransfer.2019.03.114.

[9] Tariq, A., Altaf, K., Ahmad, S. W., Hussain, G., & Ratlamwala, T. A. H. (2020). Comparative numerical and experimental analysis of thermal and hydraulic performance of improved plate fin heat sinks. *Applied Thermal Engineering*, *180*, Article 115949. https://doi.org/10.1016/j.applthermaleng.2020.115949.

[10] Bhandari, P., & Prajapati, Y. K. (2021). Thermal performance of open microchannel heat sink with variable pin fin height. *International Journal of Thermal Sciences*, *159*, Article 106609. https://doi.org/10.1016/j.ijthermalsci.2020.106609.

[11] Chamanroy, Z., & Khoshvaght-Aliabadi, M. (2019). Analysis of straight and wavy miniature heat sinks equipped with straight and wavy pin-fins. *International Journal of Thermal Sciences*, *146*, Article 106071. https://doi.org/10.1016/j.ijthermalsci.2019.106071.

[12] Kewalramani, G. V., Hedau, G., Saha, S. K., & Agrawal, A. (2019). Study of laminar single phase frictional factor and Nusselt number in In-line micro pin-fin heat sink for electronic cooling applications. *International Journal of Heat and Mass Transfer*, *138*, 796–808. https://doi.org/10.1016/j.ijheatmasstransfer.2019.04.089..

[13] Li, Y., Wang, Z., Yang, J., & Liu, H. (2020). Thermal and hydraulic characteristics of microchannel heat sinks with cavities and fins based on field synergy and thermodynamic analysis. *Applied Thermal Engineering*, *175*, Article 115348. https://doi.org/10.1016/j.applthermaleng.2020.115348.

[14] Zeng, S., Sun, Q., & Seng, P. (2020). Thermohydraulic analysis of a new fin pattern derived from topology optimized heat sink structures. *International Journal of Heat and Mass Transfer*, *147*, Article 118909. https://doi.org/10.1016/j.ijheatmasstransfer.2019.118909.

[15] Wang, X., Chen, M., Tate, D., Rahimi, H., & Zhang, S. (2020). Numerical investigation on hydraulic and thermal characteristics of micro latticed pin fin in the heat sink. *International Journal of Heat and Mass Transfer*, *149*, Article 119157. https://doi.org/10.1016/j.ijheatmasstransfer.2019.119157.

[16] Soleymani, Z., Rahimi, M., Gorzin, M., & Pahamli, Y. (2020). Performance analysis of hotspot using geometrical and operational parameters of a microchannel pin-fin hybrid heat sink. *International Journal of Heat and Mass Transfer*, *159*, Article 120141. https://doi.org/10.1016/j.ijheatmasstransfer.2020.120141.

[17] Jonsson, H., & Bjorn, P. (1996). Experimental comparison of different heat sink designs for cooling of electronics. *ASME Journal of Heat Transfer*, *329*(7), 27–34.

[18] Wirtz, R. A., Sohal, R., & Wang, H. (1997). Thermal performance of pin-fin fan-sink assemblies. *Journal of Electronic Packaging*, *119*(1), 26–31.

[19] Laor, K., & Kalman, H. (1992). Performance and temperature distributions in different fins with uniform and nonuniform heat generation. *Institution of Chemical Engineers Symposium Series*, *1*(129), 335–342.

[20] Mokheimer, E. M. A. (2002). Performance of annular fins with different profiles

Online ISSN 3007-3197
Print ISSN 3007-3189

subject to variable heat transfer coefficient. *International Journal of Heat and Mass Transfer*, *45*(17), 3631–3642. https://doi.org/10.1016/S0017-9310(02)00075-6.

[21] Ahmadian-Elmi, M., Mashayekhi, A., Nourazar, S. S., & Vafai, K. (2021). A comprehensive study on parametric optimization of the pin-fin heat sink to improve its thermal and hydraulic characteristics. *International Journal of Heat and Mass Transfer*, *180*, Article 121797. https://doi.org/10.1016/j.ijheatmasstransfer.2021.121797.